

WEIGEL, D., VEYSSEYRE, R. & PHAN, T. (1984). *C. R. Acad. Sci.* **298**, 825–828.

WOLFF, P. M. DE, JANSSEN, T. & JANNER, A. (1981). *Acta Cryst.* **A37**, 625–636.

YAMAMOTO, A. (1982a). *Acta Cryst.* **A38**, 87–92.

YAMAMOTO, A. (1982b). *REMOS*. A computer program for the refinement of modulated structures. National Institute for Research in Inorganic Materials, Niihari-gun, Ibaraki, Japan.

*Acta Cryst.* (1988). **B44**, 116–120

## Structures of the ZrO<sub>2</sub> Polymorphs at Room Temperature by High-Resolution Neutron Powder Diffraction

BY C. J. HOWARD

*Australian Nuclear Science and Technology Organisation, Lucas Heights Research Laboratories,  
Private Mail Bag 1, Menai, New South Wales 2234, Australia*

R. J. HILL

*CSIRO Division of Mineral Chemistry, PO Box 124, Port Melbourne, Victoria 3207, Australia*

AND B. E. REICHERT

*Research Group, ICI Australia Operations Pty Ltd, Newsom Street, Ascot Vale, Victoria 3032, Australia*

(Received 7 July 1987; accepted 14 October 1987)

### Abstract

The crystal structures of monoclinic ZrO<sub>2</sub> [*P2<sub>1</sub>/c*,  $a = 5.1505(1)$ ,  $b = 5.2116(1)$ ,  $c = 5.3173(1)$  Å,  $\beta = 99.230(1)^\circ$ ,  $V = 140.88(1)$  Å<sup>3</sup>,  $Z = 4$ ,  $R_{wp} = 0.047$ ], tetragonal Zr<sub>0.935</sub>Y<sub>0.065</sub>O<sub>1.968</sub> [*P4<sub>2</sub>/nmc*,  $a = 3.6055(1)$ ,  $c = 5.1797(2)$  Å,  $V = 67.33(1)$  Å<sup>3</sup>,  $Z = 2$ ,  $R_{wp} = 0.090$ ] and cubic Zr<sub>0.875</sub>Mg<sub>0.125</sub>O<sub>1.875</sub> [*Fm3m*,  $a = 5.0858(1)$  Å,  $V = 131.55(1)$  Å<sup>3</sup>,  $Z = 4$ ,  $R_{wp} = 0.083$ ] have been refined by Rietveld analysis of 1.377 Å neutron powder diffraction data collected at 295 K. In both tetragonal and cubic ZrO<sub>2</sub>, the stabilizer atoms randomly occupy the Zr site and charge balance is achieved by an appropriate number of vacancies on the O site. In cubic ZrO<sub>2</sub>, the anions are displaced from their ideal fluorite positions by 0.025*a* in the [111] direction and there is evidence for the presence of either a small quantity of a tetragonal impurity phase, or a slight tetragonal distortion.

### Introduction

Pure zirconia, ZrO<sub>2</sub>, is monoclinic at room temperature, tetragonal between ~1440 and ~2640 K, and cubic up to the melting point at ~2950 K. The monoclinic phase is a distortion of the fluorite (CaF<sub>2</sub>) structure with the Zr atom in seven coordination. In both high-temperature phases, the Zr atom assumes eight coordination, as in fluorite, but in the tetragonal form the O atom is substantially displaced from its ideal fluorite  $\frac{1}{4}, \frac{1}{4}, \frac{1}{4}$  position. The tetragonal and cubic phases of pure zirconia can be stabilized at room temperature by the addition of suitable oxides, namely MgO, CaO,

Sc<sub>2</sub>O<sub>3</sub>, Y<sub>2</sub>O<sub>3</sub> and certain rare-earth oxides. An orthorhombic form has also been prepared by quenching from high pressure and temperature (Suyama, Ashida & Kume, 1985) but this phase will not be considered further here.

The crystal structures of, and mechanisms of the transformations between, the monoclinic, tetragonal and cubic phases are of considerable technical interest since they can be manipulated to provide optimized physical and chemical properties of the materials fabricated from the stabilized zirconia (Garvie, Hannink & Pascoe, 1975; Roth, 1975; Claussen, Ruhle & Heuer, 1984; Fisher, 1986). The so-called partially stabilized zirconias (PSZ), which are typically two-phase cubic and tetragonal or single-phase tetragonal, are of importance for mechanical and structural applications. The fully stabilized zirconias (FSZ), which are normally single-phase cubic, are of interest for heating elements, oxygen sensors and fuel-cell applications.

Crystal structure determinations have been performed on tetragonal ZrO<sub>2</sub> using X-ray powder diffraction intensities collected at 1470 to 2230 K by Teufer (1962). Monoclinic ZrO<sub>2</sub> (baddeleyite) has been studied at room temperature using X-ray single-crystal methods by McCullough & Trueblood (1959) and Smith & Newkirk (1965). Cubic Zr(Ca,Y)O<sub>2-x</sub> solid solutions have been analyzed at various temperatures from both X-ray and neutron data by Carter & Roth (1968), Steele & Fender (1974), Faber, Mueller & Cooper (1978), Morinaga, Cohen & Faber (1979) and Horiuchi, Schultz, Leung & Williams (1984).

The present study gives new refinements of the crystal structures and compositions of the three ZrO<sub>2</sub> polymorphs from high-resolution neutron powder diffraction data collected at room temperature. The results provide the background to a longer-term structural and phase-analytical investigation of PSZ materials using both neutron and X-ray powder diffraction data; these latter studies will be presented elsewhere.

### Experimental

The samples used for data collection were all prepared from zirconia containing the natural amount of hafnium (about 2% by weight). The monoclinic sample was a commercial zirconia powder (Z-Tech Corporation, grade EF-Premium) prepared from zircon by a plasma dissociation process and heated to 1270 K for 80 h to increase the crystallite size. It consisted entirely of the monoclinic form and was contained in a 12 × 50 mm vanadium can for data collection.

Data for the other phases were collected on free-standing, sintered specimens of polycrystalline zirconia containing Y<sub>2</sub>O<sub>3</sub> (for the tetragonal phase) or MgO (cubic) as stabilizer. Phase-pure tetragonal ZrO<sub>2</sub> was made by pressing a commercial coprecipitated powder containing 3 mol.% Y<sub>2</sub>O<sub>3</sub> (Toyo Soda, grade TZ-3YA) into the desired shape and size for neutron diffraction data collection (a cylinder of diameter ~12 mm) followed by sintering at 1770 K. The cubic specimen was prepared by mixing a commercial monoclinic ZrO<sub>2</sub> powder (Magnesium Elektron) with 11.5 mol.% MgO, followed by milling, drying, pressing and sintering at 1970 K.

Diffraction data for all samples were recorded at 295 K on the eight-counter, fixed-wavelength, high-resolution powder diffractometer (HRPD) at the Australian Nuclear Science and Technology Organisation's research reactor HIFAR at the Lucas Heights Research Laboratories. This instrument (in an earlier single-counter configuration) has been described by Howard, Ball, Davis & Elcombe (1983). The data were recorded under monitor control at intervals of 0.05° 2θ over the angular ranges shown in Table 1, using a wavelength of 1.377 Å. The scattering lengths used for Zr, O, Mg and Y were 7.166 (modified from 7.160 to account for the presence of Hf), 5.805, 5.375 and 7.75 fm, respectively.

The least-squares structure and profile refinements were performed with the Rietveld analysis program *LHPM1* described by Hill & Howard (1986). The background was defined by a four-parameter polynomial in 2θ<sup>n</sup>, where *n* had values between 0 and 3, and was refined simultaneously with the unit-cell, zero-point, scale, peak-width/shape/asymmetry and crystal structure parameters. The peak shape was Voigtian, with the widths of the Gaussian and Lorentzian components coded to vary in accordance with the

Table 1. Summary of phase, data-collection and refinement details for ZrO<sub>2</sub>

	Monoclinic	Tetragonal	Cubic
Formula	ZrO <sub>2</sub>	Zr <sub>0.933</sub> Y <sub>0.065</sub> O <sub>1.968</sub>	Zr <sub>0.875</sub> Mg <sub>0.125</sub> O <sub>1.875</sub>
Space group	<i>P</i> 2 <sub>1</sub> / <i>c</i>	<i>P</i> 4 <sub>2</sub> / <i>nm</i> c	<i>Fm</i> 3 <i>m</i>
Crystallite size (Å)	1080 (30)	1600 (60)	1970 (80)
R.m.s. strain (%) <sup>*</sup>	0.049 (1)	0.071 (2)	0.008 (2)
Wavelength (Å)	1.377	1.377	1.377
2θ scan range (°)	12–160	10–160	10–160
Max. step intensity <sup>†</sup>	650	1230	1590
No. of unique reflections	473	68	22
No. of structural parameters <sup>‡</sup>	16	6	5§
No. of profile parameters	9	9	9
R <sub>wp</sub> (%) <sup>c</sup>	4.66	8.98	8.34
Gof <sup>c</sup>	1.85	3.34	3.17
R <sub>B</sub> (%) <sup>¶</sup>	1.95	3.50	1.64

<sup>\*</sup> Root-mean-square strain based on an assumed Gaussian distribution.

<sup>†</sup> Represents the average number of counts collected in each of eight detectors.

<sup>‡</sup> Includes atomic position, occupancy and displacement parameters and unit-cell dimensions.

<sup>§</sup> Includes a parameter associated with [111] O-atom displacement; model 3 in Table 4.

<sup>¶</sup> Standard Rietveld analysis agreement index (Young, Prince & Sparks, 1982).

Caglioti, Paoletti & Ricci (1958) function (to model the effects of particle strain and the inherent broadening due to the instrument) and with sec θ (to describe crystallite-size effects), respectively; the results of these size and strain determinations are given in Table 1. The calculated peak intensity was distributed over five peak full-widths at half-maximum on either side of the peak centre. Peak asymmetry was modelled by a sum of five Voigtians.

In the case of the tetragonal and cubic ZrO<sub>2</sub> samples, the final refinements included an examination of various models for the location of the stabilizer elements and the structural distortions associated with their incorporation; these models are discussed below. Convergence was assumed to have been achieved when the parameter shifts in the final cycle of refinement were less than ten percent of the associated estimated standard deviation (e.s.d.). The observed neutron powder diffraction profiles for the samples have been deposited\* and the plot outputs from the Rietveld analyses of the three diffraction patterns are given in Fig. 1. The final values for the refinement agreement indices are given in Table 1 and a summary of the structural and bonding parameters is presented in Tables 2–5.

### Discussion

#### Monoclinic ZrO<sub>2</sub>

Refinement of the monoclinic ZrO<sub>2</sub> structure was undertaken in space group *P*2<sub>1</sub>/*c* with all atoms in general positions. The results are shown in Table 2,

\* Lists of the observed step-scan neutron diffraction data for all samples have been deposited with the British Library Document Supply Centre as Supplementary Publication No. SUP 44455 (13 pp.). Copies may be obtained through The Executive Secretary, International Union of Crystallography, 5 Abbey Square, Chester CH1 2HU, England.

Table 2. Fractional atomic coordinates and isotropic displacement parameters for monoclinic ZrO<sub>2</sub>

	Present work	Smith & Newkirk (1965)
Zr <i>x</i>	0.2754 (2)	0.2758 (2)
<i>y</i>	0.0395 (2)	0.0411 (2)
<i>z</i>	0.2083 (2)	0.2082 (2)
<i>B/B</i> <sub>eq</sub> (Å <sup>2</sup> )	0.33 (2)	0.303
O1 <i>x</i>	0.0700 (3)	0.0703 (15)
<i>y</i>	0.3317 (3)	0.3359 (14)
<i>z</i>	0.3447 (3)	0.3406 (13)
<i>B/B</i> <sub>eq</sub> (Å <sup>2</sup> )	0.55 (2)	0.317
O2 <i>x</i>	0.4496 (3)	0.4423 (15)
<i>y</i>	0.7569 (3)	0.7549 (14)
<i>z</i>	0.4792 (3)	0.4789 (13)
<i>B/B</i> <sub>eq</sub> (Å <sup>2</sup> )	0.46 (2)	0.229

Table 3. Fractional atomic coordinates and isotropic displacement parameters for tetragonal ZrO<sub>2</sub>

	Present work	Teufer (1962)
Zr Y occupancy (%)	6.5 (21)	0
<i>B</i> (Å <sup>2</sup> )	0.65 (2)	1.66
O1 vacancies (%)	1.6	0
<i>z</i>	0.4587 (2)	0.435
<i>B</i> (Å <sup>2</sup> )	0.98 (2)	3.11

Table 4. Fractional atomic coordinates and isotropic displacement parameters for cubic ZrO<sub>2</sub>

	Model 1: O atom not displaced	Model 2: O displaced along [100]	Model 3: O displaced along [111]
Zr Mg occupancy (%)	9.6 (34)	12.5 (33)	12.5 (29)
<i>B</i> (Å <sup>2</sup> )	1.54 (3)	1.54 (3)	1.54 (3)
O1 vacancies (%)	4.8	6.5	6.5
coordinate	0.25	0.2976 (31)	0.2749 (6)
<i>B</i> (Å <sup>2</sup> )	3.15 (5)	1.43 (25)	1.73 (9)
<i>R</i> <sub>wp</sub> (%)	8.51	8.50	8.34
<i>R</i> <sub>g</sub> (%)	2.55	2.42	1.64

Table 5. Bond lengths (Å) in the ZrO<sub>2</sub> polymorphs

Monoclinic	Tetragonal	Cubic
Zr–O1 2.052 (2)	Zr–O1 2.1020 (6) × 4	Model 1:
O1 2.063 (2)	O1 2.3509 (7) × 4	Zr–O 2.2022 × 8
O2 2.153 (2)	Average = 2.226	Model 2:
O1 2.157 (2)		Zr–O 2.072 (8) × 4
O2 2.176 (2)		2.350 (10) × 4
O2 2.242 (2)		Average = 2.211
O2 2.267 (2)		Model 3:
Average = 2.159		Zr–O 2.139 (3) × 6
		2.422 (3) × 2
		Average = 2.210

where they are compared with the values obtained by Smith & Newkirk (1965) from single-crystal X-ray data. The *y* coordinate of Zr and the *x* coordinate of O2 differ by 3.8 and 4.1 combined e.s.d.'s, respectively, for the two determinations; the other coordinates are within 2.5 combined e.s.d.'s. The O coordinates are determined more precisely in the case of the neutron data refinement, as expected.

The crystal structure is a distortion of the cubic fluorite type (Smith & Newkirk, 1965). The Zr atom is in sevenfold coordination, with Zr–O distances ranging from 2.052 (2) to 2.267 (2) Å; the O1 atom is coordinated by three Zr atoms in an approximately planar configuration, while O2 is surrounded by a distorted tetrahedron of Zr atoms. There are no important differences in bond length between the present and earlier studies (Table 5).

#### Tetragonal Zr<sub>0.935</sub>Y<sub>0.065</sub>O<sub>1.968</sub>

Refinement of the neutron powder diffraction data for yttria-stabilized, tetragonal ZrO<sub>2</sub> was undertaken in space group *P*4<sub>2</sub>/*nmc* (origin at a centre of symmetry) with the Zr and O atoms in special positions 2(*a*) and 4(*d*), respectively. The results are presented in Tables 3 and 5; Table 3 also contains the parameters determined by Teufer (1962) from X-ray powder diffraction (integrated intensity) data collected at 15°O K using pure (*i.e.* unstabilized) ZrO<sub>2</sub>.

Several models for the incorporation of Y<sub>2</sub>O<sub>3</sub> into the structure were examined; the best results were achieved with Y substituting randomly for Zr, accompanied by a charge-compensating number of vacancies on the O-atom site. The least-squares determination of the Y

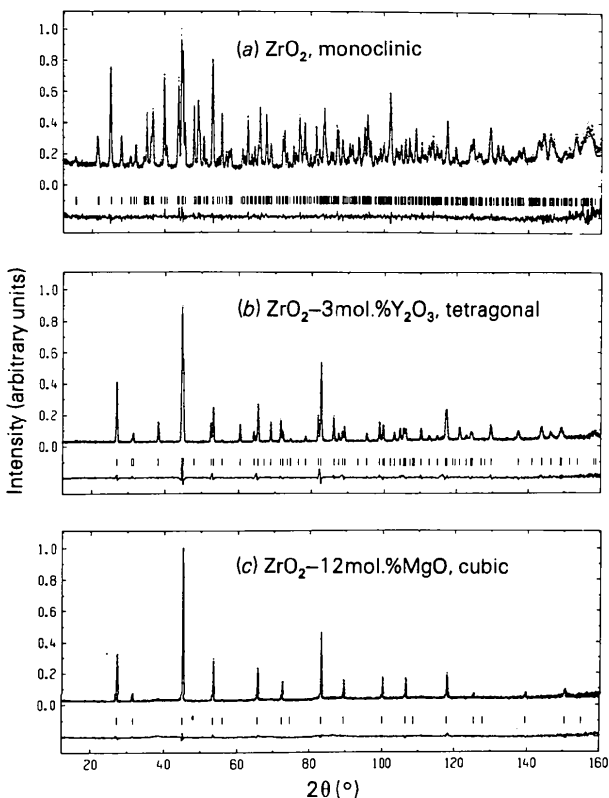


Fig. 1. Output from Rietveld analyses of the diffraction patterns from (a) monoclinic, (b) tetragonal, and (c) cubic ZrO<sub>2</sub>. The observed data are indicated by crosses and the calculated profile is the continuous line overlying them. The short vertical lines below the pattern represent the positions of all possible Bragg reflections, and the lower curve is the difference between the observed and calculated intensity at each step, plotted on the same scale.

content of the Zr site (Table 3) is in reasonable agreement with the figure derived from the chemistry of the starting material (*viz.* 5.8 atom%), although the error in the determination is large. (Note that all formulae cited in the text and tables correspond to those determined from the neutron data refinements rather than from chemical measurements.) The values of root-mean-square strain derived by deconvolution of the peak widths into their Gaussian and Lorentzian components (Table 1) provide no evidence for the presence of significant crystallite strain, despite the presence of the stabilizer cations and the fact that the polymorph is well out of its stability field in  $T$ - $X$  space (Fisher, 1986).

The one variable O-atom coordinate is significantly different from the value determined by Teufer (1962), and the thermal parameters of both O and Zr are approximately one-third of the earlier values. Some, if not all, of these differences can be attributed to the fact that the Teufer material did not contain a stabilizer and the diffraction data were collected at elevated temperature (1520 K).

#### Cubic $Zr_{0.875}Mg_{0.125}O_{1.875}$

Structure refinement results obtained for magnesia-stabilized, cubic  $ZrO_2$  are given in Tables 4 and 5; in this polymorph the Zr and O atoms are (ideally) in the special positions 4(*a*) and 8(*c*), respectively, of space group  $Fm\bar{3}m$ . Comparisons with the earlier work of Carter & Roth (1968), Steele & Fender (1974), Faber *et al.* (1978), Morinaga *et al.* (1979) and Horiuchi *et al.* (1984) are difficult to make because of the variety of preparative methods and the different kind and content of stabilizers used. Indeed, it is likely that the detailed structure of this phase is a sensitive function of its composition and preparation history. Nevertheless, the earlier studies all suggest that the anions are located in one or other or all of sites 8(*c*) at  $\frac{1}{2}, \frac{1}{2}, \frac{1}{2}$ , 32(*f*) at  $\frac{1}{4}+d, \frac{1}{4}+d, \frac{1}{4}+d$  and 48(*g*) at  $\frac{1}{4}+d, \frac{1}{4}, \frac{1}{4}$  (Horiuchi *et al.* provide a brief summary of the previous work). It has also been proposed that the stabilizer cations substitute randomly for Zr (with an appropriate number of charge-compensating vacancies on the anion site), and that these cations are displaced in the direction [111] from their ideal location at the unit-cell origin.

Various structural models for the incorporation of Mg and for the accompanying structural relaxation effects were also examined exhaustively in the present study. With the anions located in 8(*c*), the Mg content of the Zr site (assumed to be random) was determined to be  $9 \pm 3$  atom%, in reasonable agreement with the value expected from the chemical preparation (11.5 atom%); this is model 1 in Table 4. Attempts to locate the Mg in the interstitial site 4(*a*) at  $\frac{1}{2}, \frac{1}{2}, \frac{1}{2}$  resulted in zero derived occupancy and poorer values for the agreement indices.

A large value for the isotropic thermal displacement parameter of the O atom is characteristic of refinements undertaken here (Table 4) and in all earlier work, irrespective of whether the data were collected at room or at elevated temperature. It provides strong evidence for the presence of a significant displacement of the anions away from the ideal fluorite 8(*c*) positions, which does not result in the presence of significant crystallite strain (Table 1). As in previous work, two primary models for this displacement were tested: an O atom offset parallel to [100] (model 2) or [111] (model 3). Both refinements reduced the agreement indices and the O-atom thermal displacement parameter, and gave a value for the Mg occupancy of the Zr site closer to the chemical value (Tables 4 and 5). On balance, model 3 appears to be more satisfactory. Anion displacements parallel to [110] were successfully discounted, but rather more complex models involving the simultaneous presence of [100] and [111] displacements of either the anions or the cations (as tested by earlier workers) could not be supported by the data.

As shown in Fig. 1(*c*), the cubic  $ZrO_2$  diffraction pattern contains several very diffuse, low-intensity peaks that are not in accord with the usual  $Fm\bar{3}m$  structure. A similar set of weak peaks was reported by Steele & Fender (1974) and was interpreted by them to indicate the presence of a small amount of a tetragonal intergrowth phase. The additional peaks in Fig. 1(*c*) can be modelled equally well by a tetragonal-type distortion of the cubic structure or by a small amount of tetragonal material present as a second phase.

#### References

- CAGLIOTI, G., PAOLETTI, A. & RICCI, F. P. (1958). *Nucl. Instrum.* **3**, 223–228.
- CARTER, R. E. & ROTH, W. L. (1968). *EMF Measurements in High Temperature Systems*, edited by C. B. ALCOCK, pp. 125–144. New York: The Institute of Mining & Metallurgy.
- CLAUSSEN, N., RUHLE, M. & HEUER, A. H. (1984). Editors. *Advances in Ceramics*, Vol. 12, *Science and Technology of Zirconia II*. Columbus, Ohio: American Ceramic Society.
- FABER, J. JR, MUELLER, M. H. & COOPER, B. R. (1978). *Phys. Rev. B*, **17**, 4884–4888.
- FISHER, G. (1986). *Ceram. Bull.* **65**, 1355–1360.
- GARVIE, R. C., HANNINK, R. H. & PASCOE, R. T. (1975). *Nature (London)*, **258**, 703–704.
- HILL, R. J. & HOWARD, C. J. (1986). Australian Atomic Energy Commission Report No. M112. AAEC (now ANSTO), Lucas Heights Research Laboratories, New South Wales, Australia.
- HORIUCHI, H., SCHULTZ, A. J., LEUNG, P. C. W. & WILLIAMS, J. M. (1984). *Acta Cryst.* **B40**, 367–372.
- HOWARD, C. J., BALL, C. J., DAVIS, R. L. & ELCOMBE, M. M. (1983). *Aust. J. Phys.* **36**, 507–518.
- MCCULLOUGH, J. D. & TRUEBLOOD, K. N. (1959). *Acta Cryst.* **12**, 507–511.
- MORINAGA, M., COHEN, J. B. & FABER, J. JR (1979). *Acta Cryst.* **A35**, 789–795.
- ROTH, W. L. (1975). *Crystal Structure and Chemical Bonding in Inorganic Chemistry*, edited by C. J. M. ROOYMANS & A. RABENAV, pp. 85–102. Amsterdam: North-Holland.
- SMITH, D. K. & NEWKIRK, H. W. (1965). *Acta Cryst.* **18**, 983–991.

STEELE, D. & FENDER, B. E. F. (1974). *J. Phys. C*, **7**, 1–11.  
 SUYAMA, R., ASHIDA, T. & KUME, S. (1985). *J. Am. Ceram. Soc.*  
**68**, C314–C315.

TEUFER, G. (1962). *Acta Cryst.* **15**, 1187.  
 YOUNG, R. A., PRINCE, E. & SPARKS, R. A. (1982). *J. Appl. Cryst.*  
**15**, 357–359.

*Acta Cryst.* (1988). **B44**, 120–128

## Structural Study of Three Modulated Phases in Rb<sub>2</sub>ZnBr<sub>4</sub>

BY A. C. R. HOGERVORST†

*Laboratory of Applied Physics, Delft University of Technology, PO Box 5046, 2600 GA Delft, The Netherlands*

AND R. B. HELMHOLDT

*Netherlands Energy Research Foundation ECN, PO Box 1, 1755 AG Petten, The Netherlands*

(Received 4 August 1987; accepted 18 November 1987)

### Abstract

The crystal structures of Rb<sub>2</sub>ZnBr<sub>4</sub> at 293, 140 and 95 K have been studied using single-crystal X-ray diffraction or single-crystal neutron diffraction (for the structure at 95 K). The so-called incommensurate structure (293 K) and the two threefold superstructures (140 and 95 K) have been determined using a computer program for modulated structures. The resulting 293 K structure has space group *Pcmn*-(00 $\gamma$ )(*ss* $\bar{1}$ ). Because of conflicting symmetry evidence in the literature, several other space groups were tried, but they yielded less satisfactory results. For the other two phases, the space group *Pc2<sub>1</sub>n* was used. The *R* values are 0.08 (for 1512 main and 2654 satellite reflections), 0.12 (1494 + 3002 reflections) and 0.05 (for 502 + 980 reflections) for the structures at 293, 140 and 95 K respectively. There is no clear structural difference between the two threefold superstructure phases. The displacive modulation is strikingly similar in the three structures. It mainly consists of rotations of the rather rigid ZnBr<sub>4</sub> tetrahedra. The amplitude of the modulation functions is roughly 35% smaller in the 293 K structure than in the 95 K structure. The modulation functions of the two threefold superstructures show a strong pseudo-*Pcmn*(00 $\gamma$ )(*ss* $\bar{1}$ ) symmetry. The temperature parameters clearly reveal that librations of the tetrahedra form an important component of the thermal vibrations. Crystal data at 95 (1) K: *M<sub>r</sub>* = 555.9, *a* = 13.184 (4), *b* = 7.599 (2), *c* = 9.623 (5) Å, *V* = 964.1 Å<sup>3</sup>.

### 1. Introduction

In Rb<sub>2</sub>ZnBr<sub>4</sub> five phase transformations are observed at atmospheric pressure, at temperatures *T<sub>i</sub>* = 374, *T<sub>c</sub>*

= 190, *T<sub>3</sub>* = 112, *T<sub>4</sub>* = 77 and *T<sub>5</sub>* = 50 K [see, for example, Yamaguchi, Sawada, Takashige & Nakamura (1982) and Nomoto, Atake, Chaudhuri & Chihara (1983)]. The values found in the literature for these temperatures scatter around the above-mentioned values. Rb<sub>2</sub>ZnBr<sub>4</sub> melts at 753 K (Sawada, Shiroishi, Yamamoto, Takashige & Matsuo, 1977). The six solid phases are denoted as *N* (normal), *I* (incommensurate), *F* (ferroelectric), IV, V and VI from high to low temperatures. *T<sub>c</sub>* has a hysteresis of about 10 K. This value strongly depends on the sample: de Pater (1978) observed that part of a crystal remained in phase *I* even at 4 K, and de Boer (1984) observed that a crystal remained in phase *I* at temperatures below 100 K. No hysteresis has been observed for the other phase transitions.

In phase *N* (above *T<sub>i</sub>*) Rb<sub>2</sub>ZnBr<sub>4</sub> has the  $\beta$ -K<sub>2</sub>SO<sub>4</sub>-type structure with unit-cell dimensions *a* = 13.386 (3), *b* = 7.679 (2) and *c* = 9.753 (2) Å at 373 K (de Pater, 1979). In phase *I* (between *T<sub>i</sub>* and *T<sub>c</sub>*) the crystal structure is modulated by a displacive modulation wave with the modulation wave vector parallel to **c**\*: **q** =  $\gamma$ **c**\*. The value of  $\gamma$  is constant at 5/17 (0.294) within experimental error in the large temperature interval between *T<sub>i</sub>* and *T<sub>c</sub>* + 10 K [see de Pater (1979) and Iizumi & Gesi (1983)]. Thus, in this range the structure of the so-called incommensurate phase is commensurate (Hogervorst & de Wolff, 1982).

Below the 'lock-in' phase-transition temperature *T<sub>c</sub>* the value of  $\gamma$  is 1/3, and hence phase *F* has a threefold superstructure. It is not yet clear what happens between *T<sub>c</sub>* + 10 K and *T<sub>c</sub>*. Until recently it has been assumed that on lowering the temperature from *T<sub>c</sub>* + 10 K,  $\gamma$  increases monotonically from 0.294 to about 0.31 at *T<sub>c</sub>*, where it jumps to 1/3. Recent measurements of Iizumi & Gesi (1983), however, indicate a more complex behaviour. These measurements suggest that several extra phase transitions exist in that small temperature

† Present address: TNO Plastics and Rubber Research Institute, PO Box 71, 2600 AB Delft, The Netherlands.